Published in final edited form as:
Epilepsia. 2012 May ; 53(5): 908–921. doi:10.1111/j.1528-1167.2012.03463.x.

Abnormalities of granule cell dendritic structure are a prominent feature of the intrahippocampal kainic acid model of epilepsy despite reduced post-injury neurogenesis

Brian L. Murphy[1,2,*], **Rylon D. Hofacer**[1,2], **Christian N. Faulkner**[1], **Andreas W. Loepke**[1,2,3], and **Steve C. Danzer**[1,2,3]

[1]Department of Anesthesia, Cincinnati Children's Hospital Medical Center, Cincinnati, Ohio 45229

[2]Program in Neuroscience, University of Cincinnati, Cincinnati, OH 45237

[3]Departments of Anesthesia and Pediatrics, University of Cincinnati, Cincinnati, OH 45267

Abstract

Purpose—Aberrant plastic changes among adult-generated hippocampal dentate granule cells are hypothesized to contribute to the development of temporal lobe epilepsy. Changes include formation of basal dendrites projecting into the dentate hilus. Innervation of these processes by granule cell mossy fiber axons leads to the creation of recurrent excitatory circuits within the dentate. The destabilizing effect of these recurrent circuits may contribute to hyperexcitability and seizures. While basal dendrites have been identified in status epilepticus models of epilepsy associated with increased neurogenesis, whether similar changes are present in the intrahippocampal kainic acid model of epilepsy – which is associated with reduced neurogenesis – is not known.

Methods—In the present study, we used Thy1-YFP-expressing transgenic mice to determine whether hippocampal dentate granule cells develop hilar-projecting basal dendrites in the intrahippocampal kainic acid model. Brain sections were examined two weeks after treatment. Tissue was also examined using ZnT-3 immunostaining for granule cell mossy fiber terminals to assess recurrent connectivity. Adult-neurogenesis was assessed using the proliferative marker Ki-67 and the immature granule cell marker calretinin.

Key Findings—Significant numbers of cells with basal dendrites were found in this model, but their structure was distinct from basal dendrites seen in other epilepsy models, often ending in complex tufts of short branches and spines. Even more unusual, a subset of cells with basal dendrites had an inverted appearance, completely lacking apical dendrites. Spines on basal dendrites were found to be apposed to ZnT-3 immunoreactive puncta, suggestive of recurrent mossy fiber input. Finally, YFP-expressing abnormal granule cells did not colocalize Ki-67 or calretinin, indicating that these cells were more than a few weeks old, but were found almost exclusively in close proximity to the neurogenic subgranular zone, where the youngest granule cells are located.

Corresponding author: (Laboratory of Origin), Dr. Steve C. Danzer, 3333 Burnet Avenue, ML 2001, Cincinnati, Ohio 45229-3039, (513) 636-4526 (phone), (513) 636-7337 (fax), steve.danzer@cchmc.org.
*Current address: St. Jude Children's Research Hospital, 262 Danny Thomas Place, Department of Tumor Cell Biology, MS#350, Memphis, TN 38105

Ethical Statement: We confirm that we have read the Journal's position on issues involved in ethical publication and affirm that this report is consistent with those guidelines.

Disclosures: None of the authors has any conflict of interest to disclose

Significance—Recent studies have demonstrated in other models of epilepsy that dentate pathology develops following the aberrant integration of immature, adult-generated granule cells. Given these findings, one might predict that the intrahippocampal kainic acid model of epilepsy, which is associated with a dramatic reduction in adult neurogenesis, would not exhibit these changes. Here, we demonstrate that hilar basal dendrites are a common feature of this model, with the abnormal cells likely resulting from the disruption of juvenile granule cell born in the weeks prior to the insult. These studies demonstrate that post-injury neurogenesis is not required for the accumulation of large numbers of abnormal granule cells.

Introduction

A little over a decade ago, hippocampal granule cells with basal dendrites projecting into the dentate hilus were identified in rodents with temporal lobe epilepsy (Spigelman et al., 1998; Buckmaster and Dudek, 1999) and more recently following hypoxia-ischemia (Díaz-Cintra et al., 2009). Granule cell basal dendrites have also been observed in genetic epilepsy models (Stanfield and Cowan, 1979; Wenzel et al., 2001; Kwon et al., 2006; Ogawa et al., 2007). Granule cells in rodents typically possess only apical dendrites, so these basal processes are unusual. Of greater significance, however, by projecting into the hilus – which comprises part of the terminal field of granule cell mossy fiber axons – granule cell basal dendrites become potential targets for innervation by granule cell axons. Subsequent anatomical and electrophysiological studies have confirmed that hilar basal dendrites are innervated by mossy fiber axons (Ribak et al., 2000). Indeed, the majority of input to basal dendrites appears to come from other granule cells (Thind et al., 2008). This *de novo* creation of a recurrent excitatory pathway among granule cells is highly reminiscent of the better-characterized phenomenon of mossy fiber sprouting, in which granule cell axons project into the dentate inner molecular layer and form synapses with granule cell apical dendrites. The potential destabilizing effect of the recurrent mossy fiber pathway has long been hypothesized to contribute to epileptogenesis (for review see Sutula and Dudek, 2007), and the formation of a second recurrent excitatory pathway – via basal dendrites – could have significant implications for the development and manifestation of seizures in epilepsy as well (Morgan and Soltesz, 2008). Mossy fiber sprouting has been identified in almost all models of temporal lobe epilepsy, and is a hallmark for humans with the disease (Sutula and Dudek, 2007). Basal dendrite formation, on the other hand, has only been assessed in a handful of animal models, and the incidence of basal dendrites in humans with temporal lobe epilepsy has yet to be fully explored (Danzer, 2011).

Basal dendrites have been observed in animals rendered epileptic by perforant path stimulation and systemic administration of pilocarpine and kainic acid, all of which induce acute status epilepticus followed by the onset of spontaneous seizures weeks later. Here, we examined the intrahippocampal kainic acid (IHpKA) model of epilepsy. This widely-used model, in which nanomolar doses of kainic acid are injected unilaterally into the hippocampus, also produces acute status epilepticus and later onset of spontaneous seizures (Cavalheiro et al., 1982; Riban et al., 2002; Raedt et al., 2009). In addition, the IHpKA model is unique in that it produces profound granule cell dispersion. Granule cell dispersion occurs when the normal dense packing of granule cell somata is disrupted as granule cells move away from each other. Granule cell dispersion is commonly observed in patients with temporal lobe epilepsy (Houser, 1990; Mathern et al., 1997; Freiman et al., 2011), and thus modeling this particular feature may have clinical relevance. While modest dispersion has been described in other models of epilepsy (Shibley and Smith, 2002; Jessberger et al., 2005), the IHpKA model produces a progressive spreading of the granule cell body layer, first appearing at one-two weeks and increasing thereafter until the cell body layer is several-fold larger a few months later (Bouilleret et al., 1999; 2000; Kralic et al., 2005; Heinrich et al., 2006; Nitta et al., 2008). Determining whether basal dendrites are present

under these conditions will help to assess whether they are a common feature of temporal lobe epilepsy, or a feature that may only occur in specific animal models.

Neuronal structure in the present study was examined using Thy1-yellow fluorescent protein (YFP) expressing mice. Within the hippocampus of these animals, subsets of dentate granule cells, CA1 and CA3 pyramidal cells and small numbers of hilar mossy cells and glial cells express YFP. These animals were used to determine whether granule cells develop aberrant dendritic morphologies following intrahippocampal kainic acid injection.

Materials and Methods

Animals

Fourteen ten-to-eleven-week-old male (25–30g) Thy1-yellow fluorescent protein (YFP)-expressing mice on a C57BL/6 background were used for the present study. Animals were from the "H" line as described by Feng and colleagues (2000). All procedures conformed to National Institutes of Health and institutional guidelines for the care and use of animals.

Intrahippocampal kainic acid injection

Mice were maintained under an inhaled anesthesia mixture containing 68.5% N_2O, 30% O_2 and 1.5% isoflurane during intrahippocampal administration of kainic acid (IHpKA, n=5) or sodium chloride vehicle (IHpNaCl, n=3). An additional six mice received no injections and served as naïve controls. Kainic acid was injected into right dorsal hippocampus using a 0.5 ml Hamilton syringe with a 25-guage needle positioned 1.6 mm posterior and lateral to bregma, and 2.0 mm below the dura. A total volume of 60–70 nL of a 20 mM solution of kainic acid in 0.9% sterile NaCl (1.0–1.4 nmol kainic acid) or 0.9% sterile NaCl (vehicle) was injected over a period of one minute. After the injection, the needle was left in the hippocampus for an additional five minutes to avoid reflux along the needle track. The needle was then removed, and the scalp resealed with TissueMend II (Veterinary Products Laboratories, Phoenix, AZ). Upon recovering from anesthesia, mice were monitored for 8–10 hours for behavioral seizure activity. During this time, animals experienced mild clonic movements of the forelimbs, rotations and immobility as previously described (Bouilleret et al., 1999). These behavioral manifestations of seizures are associated with seizure activity within the hippocampus and cortex. At the end of the 8–10 hour observation period, mice were weighed and given sufficient lactated Ringers+5% dextrose (Hospira Inc, NDC No. 0409-7929-09) to return them to pre-treatment weight. Animals recovered in a 31.5°C incubator with food and water *ad libitum* for two days. Additional injections of lactated Ringers+5% dextrose were given as needed to maintain pre-treatment weight.

Two weeks after intrahippocampal kainic acid or vehicle administration, mice were overdosed with pentobarbital (100 mg/kg) and perfused with 0.1 M PBS+1U/ml heparin followed by 2.5% paraformaldehyde and 4% sucrose in PBS, pH 7.4. Naïve controls were perfused in an identical fashion. Brains were removed and post-fixed in the same fixative for 12 hours, cryoprotected in sucrose (10, 20, 30%) and snap frozen in 2-methyl-pentane cooled to −25°C. Coronal sections were cut on a cryostat at 60 μm, slide mounted and stored at −80°C.

Immunohistochemistry

Slides with up to four brain sections corresponding to bregma coordinates between – 1.82 mm to –2.30 mm (Paxinos and Franklin, 2001) were used for analysis. These coordinates are just outside the needle track (−1.60) so as to minimize any effects of surgical tissue damage. Sections were thawed in 0.1 M PBS, pH 7.4, and then incubated for one hour in blocking solution [5% normal donkey serum (Millipore, S30) or 5% normal goat serum (Invitrogen,

16210-072) plus 1% Igepal (Sigma-Aldrich, I3021) in 0.1 M PBS, and then overnight at 4°C in primary antibodies diluted in blocking solution. The following primary antibodies were used: rabbit anti-Prox1 (1:2000; Chemicon, AB5475); mouse anti-NeuN (1:100; Millipore, MAB377), rabbit anti- ZnT-3 (1:500; Synaptic Systems, 197 002); mouse anti-calretinin (1:1500; Millipore, Temecula, CA; MAB1568), rabbit anti-Ki-67 (1:100; Vector Laboratories, Burlingame, CA, VP-RM04). Slides were then rinsed in blocker and incubated for four hours at room temperature in secondary antibodies diluted in blocking solution. The following secondary antibodies were used: goat anti-rabbit AlexaFluor 594; donkey anti-rabbit AlexaFluor 647; goat anti-mouse AlexaFluor 647. All secondary antibodies were used at 1:750 and are from Invitrogen. Slides were cover-slipped using Gel/Mount (Biomeda, M01) and sealed with clear nail polish.

Confocal microscopy and data collection

All images were acquired with a Leica SP5 confocal system set up on a DMI 6000 inverted microscope equipped with 10X (NA 0.3) and 63X (NA 1.4) objectives. Neuron selection and analysis was conducted by an investigator blinded to treatment group.

Quantification of granule cell layer area

Granule cell layer area was quantified to assess granule cell layer dispersion. Area was quantified from confocal image stacks of Prox1 immunoreactivity. Image stacks were captured at 3 μm steps through the z-depth of the tissue using a 10X objective. The borders of the granule cell layer (defined by Prox1 immunolabeling of granule cells) were digitally encoded from the image files using Leica Application Suite software (2.0.0 build 1934) to generate area measurements.

Quantification of granule cell soma area and basal dendrite number

Granule cell soma area was quantified from confocal image stacks of YFP-expressing, Prox1 immunoreactive cells. Image stacks were captured at 1 μm steps through the z-depth of the tissue using a 63X oil objective. These confocal z-stacks were collected from the midpoint of the upper blade of the dentate from the left (contralateral, non-injected) and right (ipsilateral, injected) hemispheres of each IHpKA animal, and from the right hemisphere of each control. Z-stacks were then imported into Neurolucida software (version 9.10.2; Microbrightfield, Williston, VT) for quantification of granule cell soma maximum profile area. YFP expression was used to define the cell perimeter, while Prox1 immunoreactivity was used to confirm granule cell identity. A minimum of 20 brightly labeled YFP-expressing, Prox1-immunoreactive granule cells were randomly selected for reconstruction from each animal (IHpKA, 300 cells; IHpNaCl, 60 cells; Naïve, 240 cells; roughly equal splits between left and right hemispheres for each group). Z-stacks of YFP-expressing granule cells from the upper blade of the dentate gyrus were also used to determine the number of cells with basal dendrites. Randomly selected cells were scored for the presence of hilar projecting basal dendrites using Neurolucida software (IHpKA, 347 cells; IHpNaCl, 60 cells; Naïve, 240 cells). The distance between the soma of each cell and the granule cell body layer – hilar border was also determined. To avoid pseudoreplication, measures from each brain hemisphere (from each animal) were averaged to generate means for statistical analysis.

Statistics and data analysis

For all analyses, statistical significance was determined using SigmaPlot software (version 11.0) with an α of 0.05. Comparisons between two groups were determined using a t-test. Multiple group comparisons were made using a two-way ANOVA with treatment group and hemisphere as factors. A Holm-Sidak post-test was used to identify factors which differed

significantly. Specific statistical tests and P-values are noted in the results. Non-parametric analyses were used if the data failed normality or equal variance tests. Mean values ±SEM are reported.

Figure Preparation

Unless otherwise stated, all images are maximum projections exported as TIFF files and imported into Adobe Photoshop. Images were adjusted using Leica morphological erosion filter (radius=3; iterations=1). Brightness and contrast of digital images were adjusted to optimize cellular detail using Adobe Photoshop. Identical adjustments were made to all images meant for comparison.

Results

Unilateral injection of kainic acid into the dorsal hippocampus induces granule cell dispersion

Kainic acid injection produced acute behavioral seizures (repetitive unidirectional rotations, mild clonic movements of the forelimbs and occasional whole body convulsions) lasting from 8–10 hours in all five Thy1-YFP-expressing mice. Two weeks after kainic acid injection, granule cell body layer area was measured in the hemispheres ipsilateral and contralateral to the injection site from sections immunostained with the granule cell specific marker Prox1. A two-way ANOVA was conducted with treatment and hemisphere as factors. A significant interaction between factors was found (n=6 naïve control, 3 IHpNaCl and 5 IHpKA mice, $F=28.203$, total degrees of freedom [DF]=27, $p<0.001$). A Holm-Sidak post-test revealed a significant difference between hemispheres in the IHpKA group ($p<0.001$), with the ipsilateral (injected) hemisphere having a greater area (Fig.1). Contralateral and ipsilateral hemispheres were statistically identical in the naïve control ($p=0.803$) and IHpNaCl groups ($p=0.694$). Analyses of treatment group within hemisphere revealed that the ipsilateral hemisphere of IHpKA animals was significantly larger than the same hemisphere in all other groups (IHpKA vs. naïve, $p<0.001$; IHpKA vs. IHpNaCl, $p<0.001$). By contrast, the contralateral hemisphere of IHpKA animals was statistically identical to the contralateral hemisphere in naïve ($p=0.122$) and IHpNaCl groups ($p=0.116$). No differences among either hemisphere was found between naïve control and IHpNaCl groups (ipsilateral, $p=0.576$; contralateral, $p=0.757$). Finally, granule cell layer dispersion was also absent from the ventral hippocampus of the injected hemisphere (data not shown), indicating that this change is restricted to regions proximal to the injection site. This latter observation is consistent with previous studies (Kralic et al., 2005).

IHpKA induced somatic hypertrophy of Thy1-YFP-expressing dentate granule cells

Quantification of the cell body area of YFP-labeled granule cells in regions of the dentate exhibiting granule cell layer dispersion revealed a profound somatic hypertrophy (Fig.2). A two-way ANOVA examining treatment condition and hemisphere found a significant interaction between these factors (n=3 IHpNaCl and 5 IHpKA mice, $F=54.849$, $DF=15$, $p<0.001$). Further analysis with a Holm-Sidak post-test revealed a significant difference between hemispheres in the IHpKA group ($p<0.001$), with cells in the ipsilateral (injected) hemisphere being almost twice the size of their contralateral neighbors (Fig.2). Contralateral and ipsilateral hemispheres were statistically identical in the IHpNaCl group ($p=0.361$). Analyses of treatment group within hemisphere revealed that the ipsilateral hemisphere of IHpKA animals was significantly larger than the same hemisphere in the IHpNaCl group ($p<0.001$). By contrast, soma area in the contralateral hemisphere of IHpKA animals was statistically identical to the contralateral hemisphere in the IHpNaCl group ($p=0.206$).

Granule cell mossy fiber axons invade the dentate granule cell layer

Labeling of granule cell mossy fiber axons with ZnT-3 revealed axon fibers in the hippocampal granule cell layer of IHpKA mice (Fig.3). Immunoreactive terminals were also present in the inner molecular layer, although the clear band of mossy fiber axon staining in this region, which is characteristic of other models of epilepsy (Nadler, 2003), was absent at this time point. Notably, the dense accumulation of labeled terminals surrounding granule cell somata (Fig.4) suggests they may make perisomatic contacts with these cells.

Appearance of inverted granule cells with “tufted” basal dendrites

Significant numbers of YFP-expressing granule cells from the kainic acid-injected animals possessed basal dendrites projecting into the dentate hilus (Fig.5). As with granule cell dispersion and soma area, the effect of treatment was hemisphere dependent (two-way ANOVA with treatment and hemisphere as factors revealed a significant interaction, n=6 naïve control, 3 IHpNaCl and 5 IHpKA mice, $F=53.134$, $DF=27$, $p<0.001$). Basal dendrites were only found in the injected hemisphere of IHpKA animals, where 19.5±3.9% of granule cells possessed them. Basal dendrites were absent from the contralateral hemisphere in the same animals (Holm-Sidak post-test for hemisphere within IHpKA, $p<0.001$). The ipsilateral hemisphere of IHpKA animals also differed significantly from the ipsilateral hemisphere of naïve ($p<0.001$) and IHpNaCl ($p<0.001$) mice. By contrast, the contralateral hemispheres of IHpKA mice, which lacked basal dendrites, were statistically indistinguishable from the contralateral hemispheres of naïve and IHpNaCl mice (Holm-Sidak post-test, $p=1$ for all comparisons). Similarly, naïve and IHpNaCl mice were indistinguishable from each other, suggesting that anesthesia and sham surgery is not sufficient to promote basal dendrite formation, at least in the region examined.

A subset of basal dendrites in the IHpKA model of epilepsy were morphologically distinct from basal dendrites observed in other models of epilepsy. Basal dendrites in other models tend to be long and very spiny with relatively sparse branching patterns (Walter et al., 2007; Thind et al., 2008), and basal dendrites with this structure were observed in IHpKA animals (Fig. 5, A–C). In addition, however, a subset of basal dendrites from IHpKA animals ended in extremely complex “tufts” of short branches and dendritic spines (Figs.5d&6). These structures proved so complex that we did not attempt to reconstruct them. The elaborate and overlapping accumulations of short spines and branches precluded efforts to make accurate measures. Even more unusual, the apical dendritic trees of some granule cells with “tufted” basal dendrites were wholly lacking; the entire dendritic tree was constituted solely by the basal dendrite. The somata of these “inverted” granule cells, however, were still contained with the granule cell body layer, distinguishing them from hilar ectopic granule cells, which also tend to have unusual dendritic morphologies (Cameron et al., 2011; Pierce et al., 2011) and contribute to mossy fiber sprouting (Scharfman et al., 2000; Pierce et al., 2011). Among cells with basal dendrites, 27.8±9.1% exhibited this inverted phenotype, and these cells made up 5.9±3.0% of the entire granule cell population (depicted graphically for each IHpKA animal in figure 7). Three-dimensional reconstructions from z-series scans were used to confirm the absence of apical dendrites on these cells (see supplemental movie 1). While even detailed scans failed to reveal any apical dendrites on many cells with inverted morphologies (Fig.6, A–B), roughly half possessed thin apical processes that could be followed for short distances (<50μm) before disappearing completely (Fig.6, C–D). Whether these structures reflect leading growth process, vestigial apical dendrites or something else is not clear. Finally, given their unusual morphology, the neuronal and granule cell identity of cells with tufted basal dendrites and inverted dendritic trees was confirmed by colocalization with the neuron specific marker NeuN and the granule cell-specific marker Prox1, respectively (data not shown; Fig.5, D).

Spines on tufted basal dendrites are apposed to granule cell mossy fiber terminals

Basal dendrites identified in other models of epilepsy are innervated by mossy fiber axons (Ribak et al., 2000; Shapiro and Ribak, 2006; Thind et al., 2008; Murphy et al., 2011). To begin to determine whether the tufted basal dendrites described here receive similar input, sections were immunostained for ZnT-3, a zinc transporter enriched in hippocampal dentate granule cell mossy fiber terminals (Palmiter et al., 1996; Wenzel et al. 1997; McAuliffe et al., 2011). This approach led to two key observations. Firstly, ZnT-3 immunoreactive puncta clearly tracked the projection path of basal dendrites entering the hilus (Fig.8, A), such that more immunoreactive puncta were found in close proximity to the basal process relative to immediately adjacent regions. Secondly, high resolution imaging of ZnT-3 immunoreactive puncta revealed that they were apposed to YFP-expressing spines on “tufted” basal dendrites (Fig. 8, B–C), suggesting that these basal dendrites are innervated by neighboring granule cell mossy fiber axons.

Inverted granule cells and granule cells with basal dendrites are found close to the hilar border

Confocal z-series image stacks were used to determine the position of 347 randomly selected YFP-expressing granule cells from five IHpKA animals. For each cell, the distance between the soma and the granule cell layer – hilar border was determined. Granule cells that possessed apical dendrites and lacked basal dendrites were found on average 63.9±9.5 μm from the hilar border. Inverted granule cells and granule cells with both apical and basal dendrites, on the other hand, were found much closer to the hilar border, being on average 19.5±3.7 μm away ($p=0.002$, t-test on individual animal means, $n=5$ for each group).

YFP-expressing granule cells do not colocalize calretinin or Ki67

Prior studies indicate that the Thy1 promoter used to drive YFP expression does not become active until the cells are about 5 weeks old (Walter et al., 2007; Vuksic et al., 2008; Murphy and Danzer, 2011), implying that all of the YFP-expressing cells examined here are at least of this age. Co-labeling of YFP expressing granule cells with NeuN (Fig.4) and Prox1 (Fig. 5, D), which mark more mature granule cells, further suggests that YFP-expressing cells were not born after the insult. To generate additional evidence in support of this conclusion, sections from control and IHpKA-injected animals were immunostained with calretinin and Ki-67 (Fig.9). Ki-67 labels proliferating cells, while calretinin labels immature granule cells (<4 weeks). No colocalization was found between these markers and YFP under any of the experimental conditions examined (control tissue, ipsilateral and contralateral hemispheres of IHpKA mice). Thus, it is unlikely that the YFP expressing granule cells examined here were generated in the weeks following kainic acid injection. Furthermore, the number of calretinin and Ki-67 immunopositive cells was qualitatively reduced in the injected hemisphere of IHpKA mice relative to the contralateral hemisphere in the same animals and both hemispheres from control animals (Fig.9). This confirms that the overall rate of neurogenesis was decreased following kainic acid injection in this model, consistent with the findings of other investigators (Kralic et al., 2005; Heinrich et al., 2006; Ledergerber et al., 2006).

Kainic acid injection disrupts granule cell dendritic growth

Although the number of immature granule cells labeled with calretinin was substantially reduced in the injected hemisphere of IHpKA animals, small numbers of cells remained. A subset of these were likely calretinin-expressing interneurons (Mátyás et al., 2004), however, many appeared to be newborn granule cells – based on their small size, position in the dentate subgranular zone and localization in clusters with Ki-67 immunoreactive cells (Fig.9, C.2 and C.3, arrows). Active progenitors can produce many daughter cells, which are

frequently found in close proximity to one another. Examination of the morphology of remaining putative newborn granule cells revealed striking abnormalities relative to calretinin immunoreactive granule cells from the uninjected contralateral hemisphere. Specifically, while cells in the contralateral hemisphere consistently exhibited a prominent apical process projecting into the dentate molecular layer – the presumptive future apical dendrite – cells from the injected hemisphere exhibited very disorganized growth patterns, with processes projecting in all directions (Fig.10). These findings suggest that although neurogenesis is dramatically reduced following kainic acid injection, the small amount of proliferation that does continue likely produces abnormal granule cells.

Discussion

In the present study, kainic acid was injected unilaterally into the hippocampus of Thy1-YFP-expressing mice, producing behavioral seizures lasting up to 10 hours. Mice were allowed to recover for a period of two weeks before sacrifice. This time point corresponds roughly to the end of the latent period in this model, although animals can exhibit seizures sooner (Riban et al., 2002; Bragin et al., 2005; Raedt et al., 2009). Gross histological findings in the dentate gyrus were similar to previous studies, with animals exhibiting profound somatic hypertrophy, mossy fiber sprouting and dispersion of the cell body layer (Suzuki et al., 1995). Examination of YFP-expressing granule cells, however, revealed two striking pathologies which have not been previously described. Firstly, significant numbers of granule cells (20%) developed hilar basal dendrites. While basal dendrites are a feature of other epilepsy models, however, the structure of many of the basal dendrites examined here was unique. Basal dendrites in the IHpKA model frequently projected only a short distance into the hilus before terminating in highly elaborate “tufts” of short dendritic branches and spines. Spines in these tufts were observed in close apposition to large numbers of mossy fiber terminals, implying robust recurrent input. Secondly, a subset of cells with basal dendrites (here termed “inverted granule cells”) were found to lack apical dendritic trees: apical dendrites were either absent, or consisted only of short, unbranched processes which terminated within tens of microns from the soma. In addition to demonstrating that hilar basal dendrites are a prominent feature of the IHpKA model of epilepsy, the present study also reveals novel granule cell pathologies that may underlie a robust recurrent excitatory pathway in these animals.

Adult neurogenesis and the development of aberrant neuronal morphologies

In the systemic (rather than intrahippocampal) kainic acid (Jessberger et al., 2007) and pilocarpine (Walter et al., 2007; Kron et al., 2010; Murphy et al., 2011; Santos et al., 2011) models of epilepsy, basal dendrite formation appears to be largely restricted to granule cells born either shortly before (<5 weeks) or after the epileptogenic insult. Immature and newborn granule cells also appear to underlie mossy fiber sprouting in these models (Kron et al., 2010). Granule cells older than eight weeks, on the other hand, are resistant to developing these pathologies. These observations across models indicate that there is a critical period of granule cell development during which they are vulnerable to morphological disruption.

The role of immature and newborn granule cells in other models of epilepsy raises some interesting questions for the IHpKA model. While systemic kainic acid and pilocarpine models are associated with increased neurogenesis (Parent et al., 1997), creating a large pool of newborn cells vulnerable to disruption, the IHpKA model dramatically reduces neurogenesis in the injected hippocampus (Kralic et al., 2005; Heinrich et al., 2006; Ledergerber et al., 2006), presumably reducing the pool of vulnerable granule cells. The present findings are notable, therefore, in that despite reduced neurogenesis, morphologically abnormal granule cells were found in large numbers.

Previous work has demonstrated that in the IHpKA model, granule cell dispersion and changes in somatic morphology affect mature granule cells; adult neurogenesis is not required (Heinrich et al., 2006; Nitta et al., 2008). The present observation that virtually 100% of granule cells exhibit somatic hypertrophy strongly supports this interpretation, as the majority of cells in the dentate are generated in early development (Schlessinger et al., 1975; Bayer 1980a, 1980b; Altman and Bayer 1990a, 1990b). Consistent with this interpretation, the YFP-expressing cells examined here do not colocalize with the proliferative marker Ki-67 or the early granule cell marker calretinin, but do express the later neuronal markers NeuN and prox1 (for review of markers, see Hodge et al., 2008; Zhao et al., 2008). YFP-expression is also significant as a cell-age determinant in the Thy1-YFP mice used here because the Thy1 promoter does not become active in granule cells until cells are about five-weeks-old (Walter et al., 2007; Vuksic et al., 2008; Murphy and Danzer, 2011). The YFP-expressing granule cells examined in the present study, therefore, were likely at least three-weeks-old at the time of kainic acid injection.

Interestingly, cells as young as five weeks old have been shown to contribute to basal dendrite formation and mossy fiber sprouting. While not newborn, inverted granule cells and cells with tufted basal dendrites may have been in this “juvenile” stage at the time of the insult. In support of this idea, we note that cells with these abnormalities were found almost exclusively in the inner third of the granule cell body layer – close to the subgranular zone where new cells are generated and within the region where the youngest cells are found (Mathews et al., 2010). This provides circumstantial evidence that younger cells are more vulnerable to developing basal dendrites in this model. Consistent with this interpretation, small numbers of calretinin immunoreactive cells still present in the injected hippocampus frequently exhibited abnormal morphologies, suggesting that like other epilepsy models, immature cells are vulnerable to disruption in the IHpKA model. Ultimately, however, neuronal birthdating studies will be required to determine whether the conditions induced by the IHpKA model only induce young granule cells to exhibit basal dendrites and develop inverted morphologies, or whether a wider age-range can be recruited.

Mossy fiber sprouting in the IHpKA model

In accordance with previous studies (Rougier et al., 2005; Mitsuya et al., 2009), ZnT-3 staining revealed robust sprouting of mossy fiber axons in treated animals. While the classic pattern of mossy fiber sprouting targets granule cell dendrites in the inner molecular layer, at the two-week time point examined here ZnT-3 immunoreactive puncta were overwhelming found around granule cell somata. The expansion of the granule cell layer into and beyond the original location of the inner molecular layer (Figs.1 & 2) may contribute to the more irregular pattern of mossy fiber sprouting (Rougier et al., 2005). Mossy fiber sprouting can take months to fully develop (Okazaki et al., 1995), so whether sprouting in these animals would have assumed a more typical pattern at a later date is not clear. The presence of large numbers of ZnT-3 immunoreactive terminals around granule cell somata observed here, however, implies that recurrent activation via mossy fiber axons is primarily perisomatic at this time point. This is potentially significant, as perisomatic synapses can exert greater influence on neuronal firing than more distal synapses.

Summary

The implications of the present study are two-fold. Firstly, these studies add the IHpKA model of temporal lobe epilepsy to the growing list of epilepsy models in which basal dendrites are a prominent feature. Secondly, these studies reveal that the neuronal restructuring evident in temporal lobe epilepsy models need not be stereotyped. While basal dendrites are evident in both the IHpKA and pilocarpine models of epilepsy, for example, the elaborate basal dendrite “tufts” and “inverted” granule cells have only been observed

here. The extent to which these abnormal cells persist in this model, and/or whether these features reflect transitional forms remains to be determined. Nonetheless, the present findings broaden the range of abnormalities that can be exhibited by granule cells, and raise intriguing questions regarding the specific mechanisms that mediate distinct cellular changes.

Acknowledgments

This work was supported by the National Institute of Neurological Disorders and Stroke (SCD, Award Number R01NS062806). The content is solely the responsibility of the authors and does not necessarily represent the official views of the National Institute of Neurological Disorders and Stroke or the National Institutes of Health. Thy1-YFP mice were kindly provided by Dr. Guoping Feng (Duke University). We would like to thank Keri Kaeding for useful comments on earlier versions of this manuscript.

References

Altman J, Bayer SA. Migration and distribution of two populations of hippocampal granule cell precursors during the perinatal and postnatal periods. J Comp Neurol. 1990a; 301:365–81. [PubMed: 2262596]

Altman J, Bayer SA. Mosaic organization of the hippocampal neuroepithelium and the multiple germinal sources of dentate granule cells. J Comp Neurol. 1990b; 301:325–42. [PubMed: 2262594]

Bayer SA. Development of the hippocampal region in the rat. I. Neurogenesis examined with 3H-thymidine autoradiography. J Comp Neurol. 1980a; 190:87–114. [PubMed: 7381056]

Bayer SA. Development of the hippocampal region in the rat. II. Morphogenesis during embryonic and early postnatal life. J Comp Neurol. 1980b; 190:115–34. [PubMed: 7381049]

Bouilleret V, Ridoux V, Depaulis A, Marescaux C, Nehlig A, Le Gal La Salle G. Recurrent seizures and hippocampal sclerosis following intrahippocampal kainate injection in adult mice: electroencephalography, histopathology and synaptic reorganization similar to mesial temporal lobe epilepsy. Neuroscience. 1999; 89:717–29. [PubMed: 10199607]

Bouilleret V, Loup F, Kiener T, Marescaux C, Fritschy JM. Early loss of interneurons and delayed subunit-specific changes in GABA(A)-receptor expression in a mouse model of mesial temporal lobe epilepsy. Hippocampus. 2000; 10:305–24. [PubMed: 10902900]

Bragin A, Azizyan A, Almajano J, Wilson CL, Engel J Jr. Analysis of chronic seizure onsets after intrahippocampal kainic acid injection in freely moving rats. Epilepsia. 2005; 46:1592–8. [PubMed: 16190929]

Buckmaster PS, Dudek FE. In vivo intracellular analysis of granule cell axon reorganization in epileptic rats. J Neurophysiol. 1999; 81:712–21. [PubMed: 10036272]

Cameron MC, Zhan RZ, Nadler JV. Morphologic integration of hilar ectopic granule cells into dentate gyrus circuitry in the pilocarpine model of temporal lobe epilepsy. J Comp Neurol. 2011; 519:2175–92. [PubMed: 21455997]

Cavalheiro EA, Riche DA, Le Gal La Salle G. Long-term effects of intrahippocampal kainic acid injection in rats: a method for inducing spontaneous recurrent seizures. Electroencephalogr Clin Neurophysiol. 1982; 53:581–9. [PubMed: 6177503]

Danzer SC. Depression, stress, epilepsy and adult neurogenesis. Exp Neurol. 2011 Jun 12. [Epub ahead of print].

Díaz-Cintra S, Xue B, Spigelman I, Van K, Wong AM, Obenaus A, Ribak CE. Dentate granule cells form hilar basal dendrites in a rat model of hypoxia-ischemia. Brain Res. 2009; 1285:182–7. [PubMed: 19539612]

Feng G, Mellor RH, Bernstein M, Keller-Peck C, Nguyen QT, Wallace M, Nerbonne JM, Lichtman JW, Sanes JR. Imaging neuronal subsets in transgenic mice expressing multiple spectral variants of GFP. Neuron. 2000; 28:41–51. [PubMed: 11086982]

Freiman TM, Eismann-Schweimler J, Frotscher M. Granule cell dispersion in temporal lobe epilepsy is associated with changes in dendritic orientation and spine distribution. Exp Neurol. 2011; 229:332–8. [PubMed: 21376037]

Heinrich C, Nitta N, Flubacher A, Müller M, Fahrner A, Kirsch M, Freiman T, Suzuki F, Depaulis A, Frotscher M, Haas CA. Reelin deficiency and displacement of mature neurons, but not neurogenesis, underlie the formation of granule cell dispersion in the epileptic hippocampus. J Neurosci. 2006; 26:4701–13. [PubMed: 16641251]

Hodge RD, Kowalczyk TD, Wolf SA, Encinas JM, Rippey C, Enikolopov G, Kempermann G, Hevner RF. Intermediate progenitors in adult hippocampal neurogenesis: Tbr2 expression and coordinate regulation of neuronal output. J Neurosci. 2008; 28:3707–17. [PubMed: 18385329]

Houser CR. Granule cell dispersion in the dentate gyrus of humans with temporal lobe epilepsy. Brain Res. 1990; 535:195–204. [PubMed: 1705855]

Jessberger S, Römer B, Babu H, Kempermann G. Seizures induce proliferation and dispersion of doublecortin-positive hippocampal progenitor cells. Exp Neurol. 2005; 196:342–51. [PubMed: 16168988]

Jessberger S, Zhao C, Toni N, Clemenson GD Jr, Li Y, Gage FH. Seizure-associated, aberrant neurogenesis in adult rats characterized with retrovirus-mediated cell labeling. J Neurosci. 2007; 27:9400–7. [PubMed: 17728453]

Kralic JE, Ledergerber DA, Fritschy JM. Disruption of the neurogenic potential of the dentate gyrus in a mouse model of temporal lobe epilepsy with focal seizures. Eur J Neurosci. 2005; 22:1916–27. [PubMed: 16262631]

Kron MM, Zhang H, Parent JM. The developmental stage of dentate granule cells dictates their contribution to seizure-induced plasticity. J Neurosci. 2010; 30:2051–9. [PubMed: 20147533]

Kwon CH, Luikart BW, Powell CM, Zhou J, Matheny SA, Zhang W, Li Y, Baker SJ, Parada LF. Pten regulates neuronal arborization and social interaction in mice. Neuron. 2006; 50:377–88. [PubMed: 16675393]

Ledergerber D, Fritschy JM, Kralic JE. Impairment of dentate gyrus neuronal progenitor cell differentiation in a mouse model of temporal lobe epilepsy. Exp Neurol. 2006; 199:130–42. [PubMed: 16624297]

Mathern GW, Kuhlman PA, Mendoza D, Pretorius JK. Human fascia dentata anatomy and hippocampal neuron densities differ depending on the epileptic syndrome and age at first seizure. J Neuropathol Exp Neurol. 1997; 56:199–212. [PubMed: 9034374]

Mathews EA, Morgenstern NA, Piatti VC, Zhao C, Jessberger S, Schinder AF, Gage FH. A distinctive layering pattern of mouse dentate granule cells is generated by developmental and adult neurogenesis. J Comp Neurol. 2010; 518:4479–90. [PubMed: 20886617]

Mátyás F, Freund TF, Gulyás AI. Immunocytochemically defined interneuron populations in the hippocampus of mouse strains used in transgenic technology. Hippocampus. 2004; 14:460–81. [PubMed: 15224983]

McAuliffe JJ, Bronson SL, Hester MS, Murphy BL, Dahlquist-Topalá R, Richards DA, Danzer SC. Altered patterning of dentate granule cell mossy fiber inputs onto CA3 pyramidal cells in limbic epilepsy. Hippocampus. 2011; 21:93–107. [PubMed: 20014385]

Mitsuya K, Nitta N, Suzuki F. Persistent zinc depletion in the mossy fiber terminals in the intrahippocampal kainate mouse model of mesial temporal lobe epilepsy. Epilepsia. 2009; 50:1979–90. [PubMed: 19389150]

Morgan RJ, Soltesz I. Nonrandom connectivity of the epileptic dentate gyrus predicts a major role for neuronal hubs in seizures. Proc Natl Acad Sci U S A. 2008; 105:6179–84. [PubMed: 18375756]

Murphy BL, Danzer SC. Somatic translocation: a novel mechanism of granule cell dendritic dysmorphogenesis and dispersion. J Neurosci. 2011; 31:2959–64. [PubMed: 21414917]

Murphy BL, Pun RY, Yin H, Faulkner CR, Loepke AW, Danzer SC. Heterogeneous integration of adult-generated granule cells into the epileptic brain. J Neurosci. 2011; 31:105–17. [PubMed: 21209195]

Nadler JV. The recurrent mossy fiber pathway of the epileptic brain. Neurochem Res. 2003; 28:1649–58. [PubMed: 14584819]

Nitta N, Heinrich C, Hirai H, Suzuki F. Granule cell dispersion develops without neurogenesis and does not fully depend on astroglial cell generation in a mouse model of temporal lobe epilepsy. Epilepsia. 2008; 49:1711–22. [PubMed: 18397295]

Ogawa S, Kwon CH, Zhou J, Koovakkattu D, Parada LF, Sinton CM. A seizure-prone phenotype is associated with altered free-running rhythm in Pten mutant mice. Brain Res. 2007; 1168:112–23. [PubMed: 17706614]

Okazaki MM, Evenson DA, Nadler JV. Hippocampal mossy fiber sprouting and synapse formation after status epilepticus in rats: visualization after retrograde transport of biocytin. J Comp Neurol. 1995; 352:515–34. [PubMed: 7721998]

Palmiter RD, Cole TB, Quaife CJ, Findley SD. ZnT-3, a putative transporter of zinc into synaptic vesicles. Proc Natl Acad Sci U S A. 1996; 93:14934–9. [PubMed: 8962159]

Parent JM, Yu TW, Leibowitz RT, Geschwind DH, Sloviter RS, Lowenstein DH. Dentate granule cell neurogenesis is increased by seizures and contributes to aberrant network reorganization in the adult rat hippocampus. J Neurosci. 1997; 17:3727–38. [PubMed: 9133393]

Paxinos, G.; Franklin, KB. The Mouse Brain in Stereotaxic Coordinates. Academic Press; London: 2001.

Pierce JP, McCloskey DP, Scharfman HE. Morphometry of hilar ectopic granule cells in the rat. J Comp Neurol. 2011; 519:1196–218. [PubMed: 21344409]

Raedt R, Van Dycke A, Van Melkebeke D, De Smedt T, Claeys P, Wyckhuys T, Vonck K, Wadman W, Boon P. Seizures in the intrahippocampal kainic acid epilepsy model: characterization using long-term video-EEG monitoring in the rat. Acta Neurol Scand. 2009; 119:293–303. [PubMed: 19388152]

Ribak CE, Tran PH, Spigelman I, Okazaki MM, Nadler JV. Status epilepticus-induced hilar basal dendrites on rodent granule cells contribute to recurrent excitatory circuitry. J Comp Neurol. 2000; 428:240–53. [PubMed: 11064364]

Riban V, Bouilleret V, Pham-Lê BT, Fritschy JM, Marescaux C, Depaulis A. Evolution of hippocampal epileptic activity during the development of hippocampal sclerosis in a mouse model of temporal lobe epilepsy. Neuroscience. 2002; 112:101–11. [PubMed: 12044475]

Rougier A, Arthaud S, Zombre N, La Salle Gle G. Patterns of dentate granule cell responses to perforant path stimulation in epileptic mice with granule cell dispersion. Epilepsy Res. 2005; 63:119–29. [PubMed: 15777666]

Santos VR, de Castro OW, Pun RY, Hester MS, Murphy BL, Loepke AW, Garcia-Cairasco N, Danzer SC. Contributions of mature granule cells to structural plasticity in temporal lobe epilepsy. Neuroscience. 2011; 197:348–57. [PubMed: 21963349]

Schlessinger AR, Cowan WM, Gottlieb DI. An autoradiographic study of the time of origin and the pattern of granule cell migration in the dentate gyrus of the rat. J Comp Neurol. 1975; 159:149–75. [PubMed: 1112911]

Scharfman HE, Goodman JH, Sollas AL. Granule-like neurons at the hilar/CA3 border after status epilepticus and their synchrony with area CA3 pyramidal cells: functional implications of seizure-induced neurogenesis. J Neurosci. 2000; 20:6144–58. [PubMed: 10934264]

Shapiro LA, Ribak CE. Newly born dentate granule neurons after pilocarpine-induced epilepsy have hilar basal dendrites with immature synapses. Epilepsy Res. 2006; 69:53–66. [PubMed: 16480853]

Shibley H, Smith BN. Pilocarpine-induced status epilepticus results in mossy fiber sprouting and spontaneous seizures in C57BL/6 and CD-1 mice. Epilepsy Res. 2002; 49:109–20. [PubMed: 12049799]

Spigelman I, Yan XX, Obenaus A, Lee EY, Wasterlain CG, Ribak CE. Dentate granule cells form novel basal dendrites in a rat model of temporal lobe epilepsy. Neuroscience. 1998; 86:109–20. [PubMed: 9692747]

Stanfield BB, Cowan WM. The morphology of the hippocampus and dentate gyrus in normal and reeler mice. J Comp Neurol. 1979; 185:393–422. [PubMed: 438366]

Sutula TP, Dudek FE. Unmasking recurrent excitation generated by mossy fiber sprouting in the epileptic dentate gyrus: an emergent property of a complex system. Prog Brain Res. 2007; 163:541–63. [PubMed: 17765737]

Suzuki F, Junier MP, Guilhem D, Sørensen JC, Onteniente B. Morphogenetic effect of kainate on adult hippocampal neurons associated with a prolonged expression of brain-derived neurotrophic factor. Neuroscience. 1995; 64:665–74. [PubMed: 7715779]

Thind KK, Ribak CE, Buckmaster PS. Synaptic input to dentate granule cell basal dendrites in a rat model of temporal lobe epilepsy. J Comp Neurol. 2008; 509:190–202. [PubMed: 18461605]

Vuksic M, Del Turco D, Bas Orth C, Burbach GJ, Feng G, Müller CM, Schwarzacher SW, Deller T. 3D-reconstruction and functional properties of GFP-positive and GFP-negative granule cells in the fascia dentata of the Thy1-GFP mouse. Hippocampus. 2008; 18:364–75. [PubMed: 18189310]

Walter C, Murphy BL, Pun RY, Spieles-Engemann AL, Danzer SC. Pilocarpine-induced seizures cause selective time-dependent changes to adult-generated hippocampal dentate granule cells. J Neurosci. 2007; 27:7541–52. [PubMed: 17626215]

Wenzel HJ, Cole TB, Born DE, Schwartzkroin PA, Palmiter RD. Ultrastructural localization of zinc transporter-3 (ZnT-3) to synaptic vesicle membranes within mossy fiber boutons in the hippocampus of mouse and monkey. Proc Natl Acad Sci U S A. 1997; 94:12676–81. [PubMed: 9356509]

Wenzel HJ, Robbins CA, Tsai LH, Schwartzkroin PA. Abnormal morphological and functional organization of the hippocampus in a p35 mutant model of cortical dysplasia associated with spontaneous seizures. J Neurosci. 2001; 21:983–98. [PubMed: 11157084]

Zhao C, Deng W, Gage FH. Mechanisms and functional implications of adult neurogenesis. Cell. 2008; 132:645–60. [PubMed: 18295581]

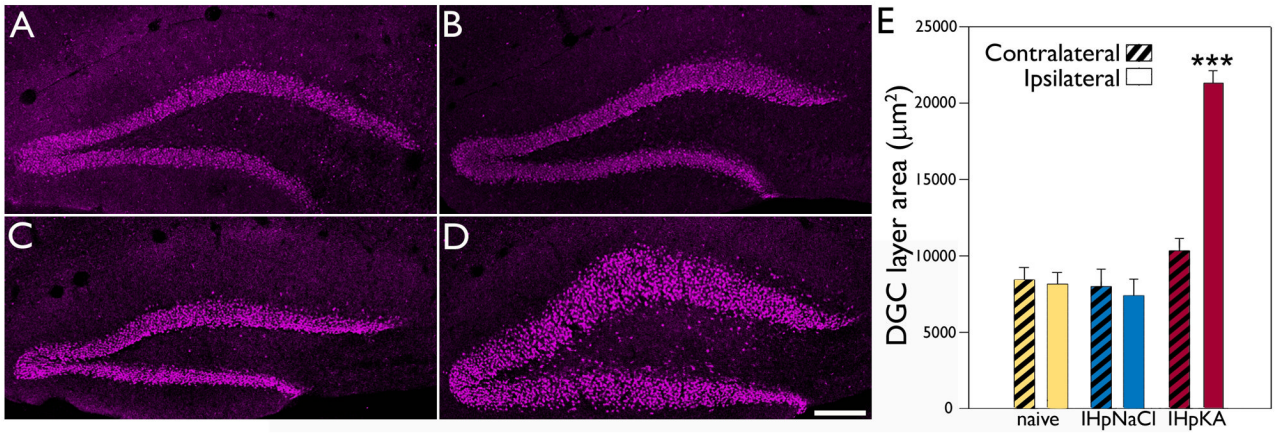

Figure 1.

Intrahippocampal injection of kainic acid leads to granule cell layer dispersion in the injected hemisphere. Representative confocal optical sections of Prox1 immunoreactivity within the dentate granule cell layer from the right hemisphere of a naïve mouse (A), ipsilateral hemisphere of an IHpNaCl mouse (B), contralateral hemisphere of an IHpKA mouse (C) and ipsilateral hemisphere of an IHpKA mouse (D). Scale bar = 100 μm. **E:** Mean area of the dentate granule cell layer by treatment group and hemisphere. Bars are means±SEM. ***P<0.001 relative to all other groups.

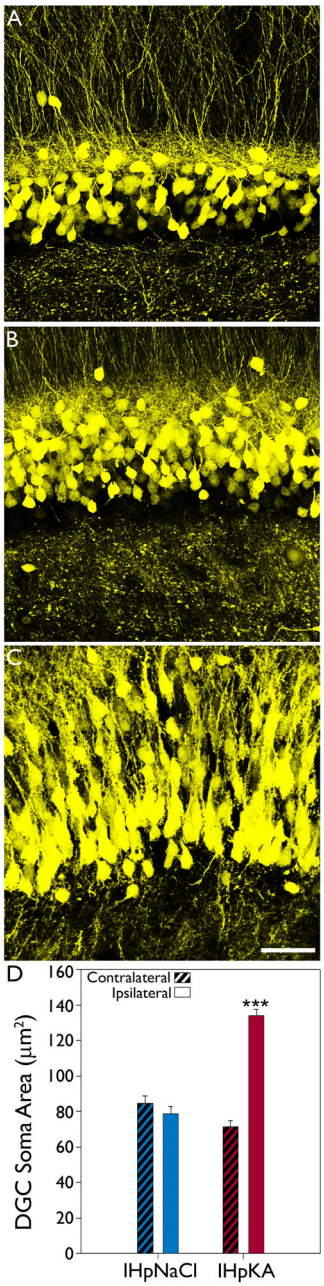

Figure 2.

Intrahippocampal injection of kainic acid induces ipsilateral granule cell somatic hypertrophy. Representative confocal maximum projections of YFP-expressing granule cells located in the upper blade of dentate gyrus from the ipsilateral hemisphere of an IHpNaCl mouse (A), contralateral hemisphere of an IHpKA mouse (B) and ipsilateral hemisphere of an IHpKA mouse (C). Note the hypertrophied granule cell somata within the ipsilateral hemisphere of the IHpKA mouse. Scale bar = 40 μm. **D:** Mean area (± SEM) of YFP-expressing granule cell somata by treatment group and hemisphere. ***P<0.001 vs. all other groups.

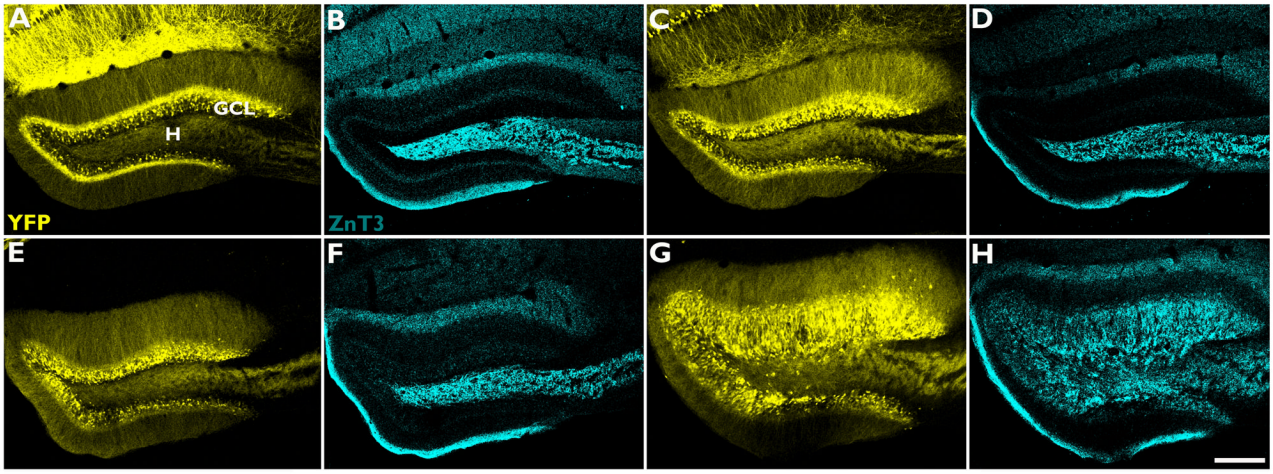

Figure 3.

The pattern of ZnT-3 immunoreactivity, a marker of mossy fiber axon terminals, is altered following intrahippocampal injection of kainic acid. Representative confocal maximum projections of YFP-expressing granule cells (yellow) and ZnT-3 immunoreactivity (cyan) within the dentate granule cell layer from the right hemisphere of a naïve mouse (A–B), ipsilateral hemisphere of an IHpNaCl mouse (C–D), contralateral hemisphere of an IHpKA mouse (E–F) and ipsilateral hemisphere of an IHpKA mouse (G–H). Note the restriction of ZnT-3 immunostaining to the hilus (H) in B, D and F, and the spread of staining into the dentate granule cell layer (GCL) in H. Scale bar = 200 μm.

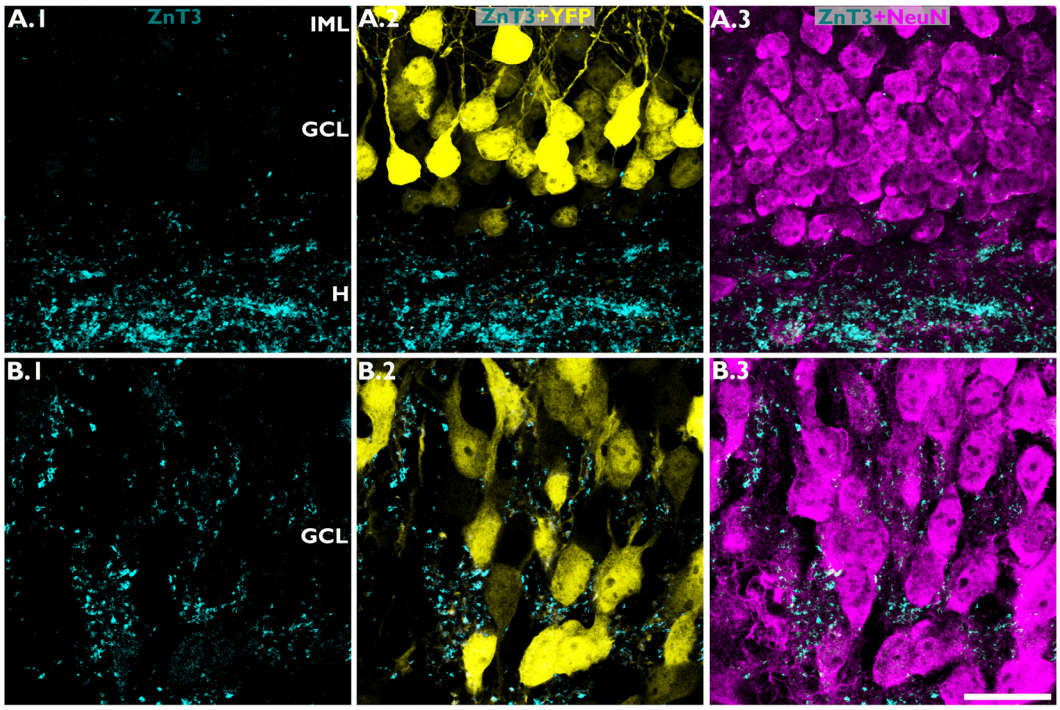

Figure 4.

ZnT-3 staining of mossy fiber axons in IHpNaCl (A) and IHpKA mice (B). ZnT-3 staining (column A.1-B.1) is shown merged with YFP (yellow) in column A.2-B.2, and NeuN (magenta) in column A.3-B.3. In IHpNaCl mice, Znt-3 staining was restricted to the dentate hilus (H), the typical projection field of mossy fiber axons. In IHpKA mice, ZnT-3 immunoreactive mossy fibers invade the dentate granule cell layer (GCL) and immunoreactive puncta were found apposed to granule cell somata. IML, inner molecular layer. Scale bar = 20 μm.

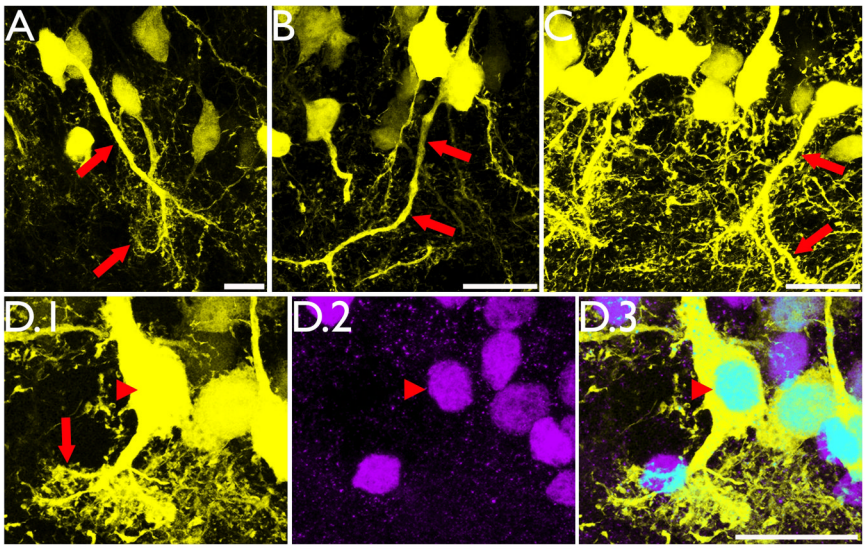

Figure 5.
Intrahippocampal injection of kainic acid results in the formation of hilar basal dendrites with structures similar to those observed in other models of epilepsy (A–C, red arrows) and novel “tufted” hilar basal dendrites (D.1, red arrow) on YFP-expressing granule cells. To confirm the granule cell identity of the cell shown in D.1, the section was co-labeled with the granule cell specific marker Prox1 (D.2). Colocalization of YFP and Prox1 is shown in D.3 (arrowhead). Images are confocal maximum projections. Scale bars = 20 μm.

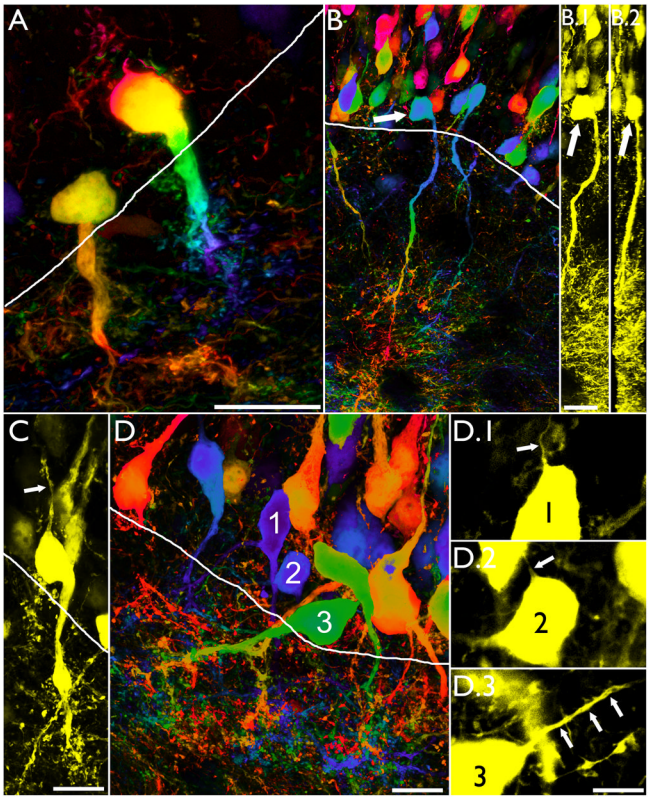

Figure 6.

Confocal maximum projections of "inverted" hippocampal granule cells from IHpKA animals. All cells shown had their somata in the granule cell body layer (white lines denote the granule cell layer – hilar border, with the former towards the top of the page). Colored images (A,B and D) were processed using a depth filter, which assigns different colors to portions of the cell located at different depths in the tissue (Leica Application Suite software). Use of this filter facilitates distinguishing individual cell features in two-dimensional projections. **A–B:** Inverted granule cells with tufted basal dendrites. Face on (0°) and 90°rotations of the cell shown in B are shown in B.1 and B.2, respectively (arrows). Rotations confirm that the soma is contained within the tissue section, and that apical process weren't missed due to artificial truncation of the soma at the slice surface. Scale bars = 20 μm. **C:** Inverted granule cell with a short apical process (arrow). Scale bar = 10 μm. **D:** Examples of three inverted granule cells with short, thin apical processes (arrows, D.1–D.3). Scale bar = 10 μm.

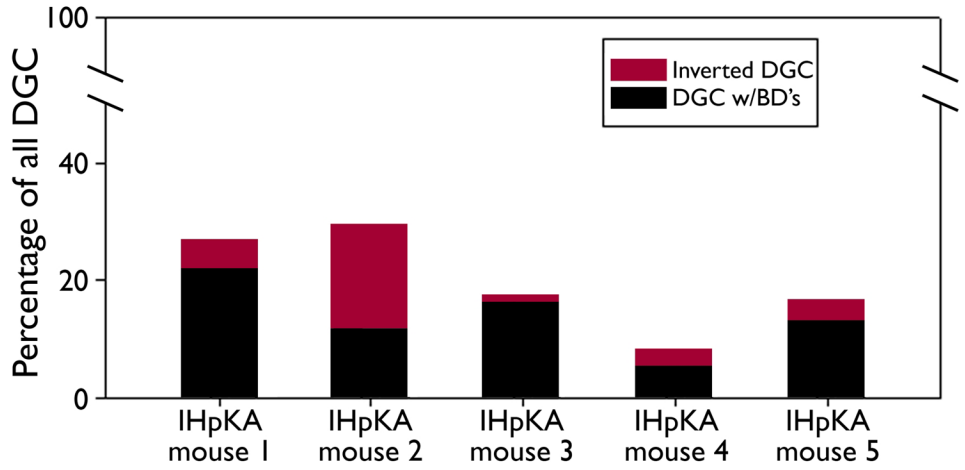

Figure 7.

Bars depict the percentage of dentate granule cells with both apical and basal dendrites (DGC w/BD's, black) and the percentage of inverted DGC (with basal dendrites only, red) in each of the five IHpKA animals. Remaining granule cells (not depicted) possessed only apical dendrites.

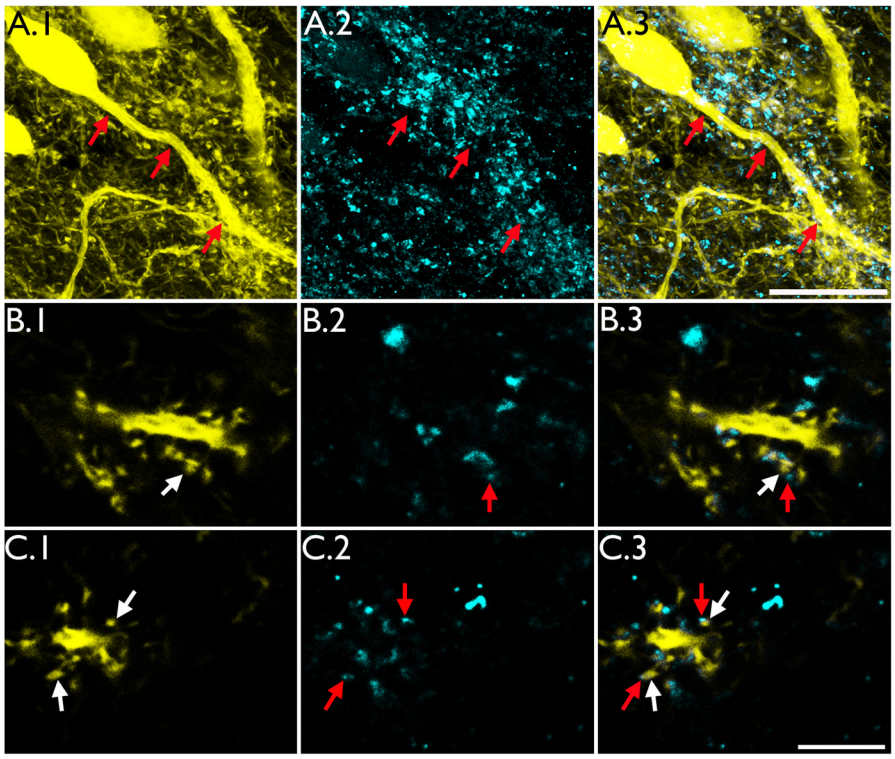

Figure 8.

ZnT-3 immunoreactive puncta were found apposed to the dendritic spines of hilar basal dendrites. **A:** Confocal maximum projections from an IHpKA animal showing a YFP-expressing hippocampal granule cell with a hilar basal dendrite. YFP-expression is shown in A.1, ZnT-3 immunoreactivity in A.2 and merged YFP expression and ZnT-3 immunoreactivity in A.3. Note the tracking of the basal process shown in A.1 by ZnT-3 immunoreactive puncta shown in A.2 (arrows). Scale bar = 20μm. **B & C:** Confocal optical sections of hilar basal dendrites showing YFP labeled dendritic spines (B.1 & C.1) apposed to ZnT-3 immunoreactive puncta (B.2 and C.2). Merged images are shown in B.3 and C.3. Paired red and white arrows denote ZnT-3 puncta apposed to labeled spines, respectively. Scale bar = 5μm.

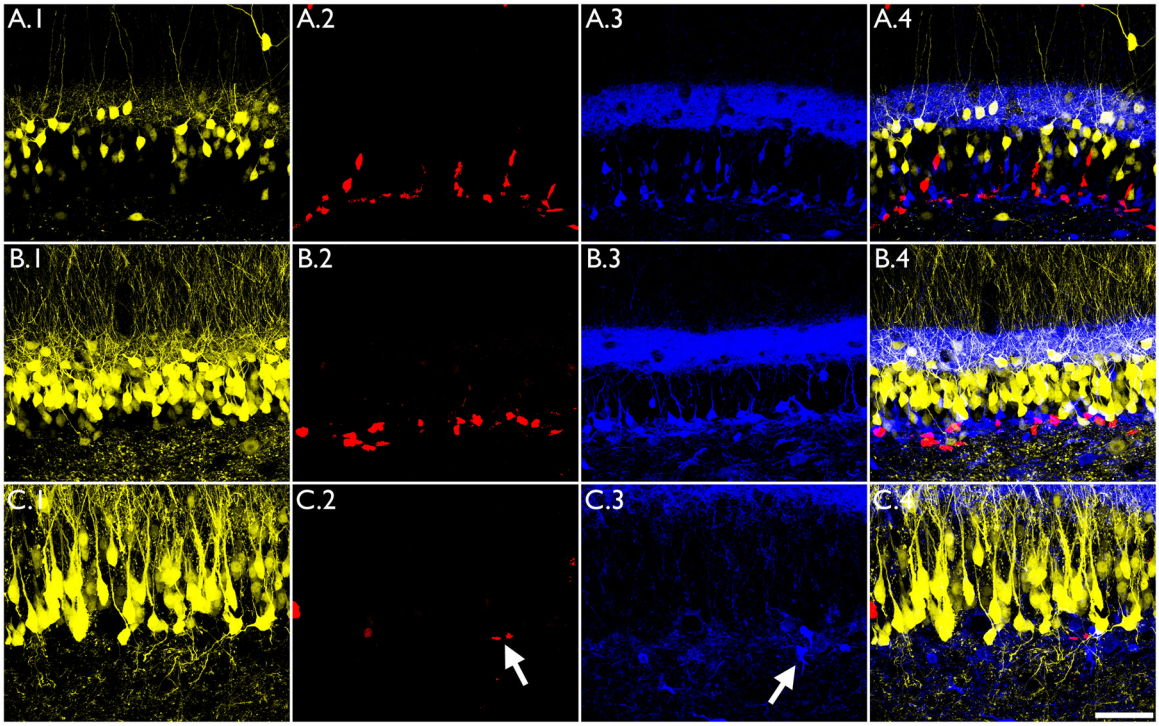

Figure 9.

The proliferative marker Ki-67 and the early granule cell marker calretinin do not colocalize with YFP-expressing granule cells in the Thy1-YFP mouse. Images show sections from the ipsilateral hemisphere of a IHpNaCl mouse (A), and the contralateral (B) and ispsilateral (C) hemispheres of IHpKA mouse. YFP expression did not colocalize with either Ki-67 (column A.2-C.2) or calretinin (column A.3-C.3) immunostaining. Merged images are shown in column A.4-C.4. Also note the reduction in the number of Ki-67 and calretinin immunoreactive cells (arrows) in the kainic acid injected hemisphere (C.2, C.3) relative to control hemispheres. Scale bar = 50μm.

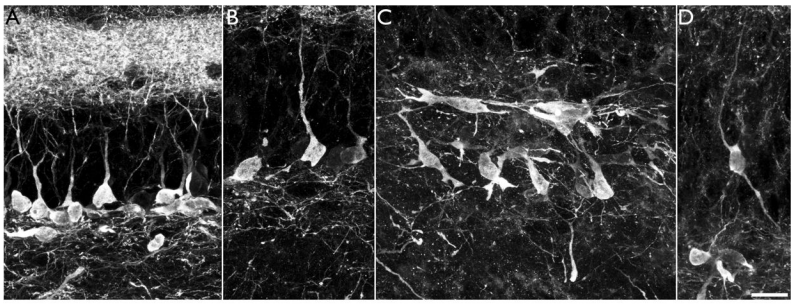

Figure 10.

In the contralateral hemisphere of IHpKA mice (A–B), calretinin-immunoreactive newborn dentate granule cells exhibited prominent apical processes projecting into the dentate molecular layer. By contrast, remaining calretinin-immunoreactive granule cells in the injected hemisphere (C–D) exhibit disorganized process projecting all directions, including into the dentate hilus. All images are confocal maximum projections. Scale bar = 15 μm.